



25th ABCM International Congress of Mechanical Engineering
October 20-25, 2019, Uberlândia, MG, Brazil

COBEM2019-1831

LOW-COST AUTOMATED POLARISCOPE FOR THE IMPLEMENTATION OF A DIDACTIC LABORATORY IN SOLID MECHANICS.

Brenda Nascimento Bandeira

Bruno Ribeiro da Luz

Mechanical Engineering Department of Federal University of Piauí

e-mails: brendabandeira2012@hotmail.com, bruno.ribeiro.da.luz@gmail.com

Alexandre de Castro Maciel

Physics Department of Federal University of Piauí

e-mail: acmaciel@ufpi.edu.br

Antônio Sales Oliveira Coelho

Mechanical Engineering Department of Federal University of Piauí

e-mail: antoniosales@ufpi.edu.br

Abstract. *It is not novelty that engineers use the transmission photoelasticity for stress analysis and observation of structures submitted to different loads. This method enables an entire field of analysis, both qualitatively and quantitatively, thus facilitating the studies and research related to Solid Mechanics widely discussed in Engineering. For the use of this technique, an instrument called polariscope is required. It can use either planar or circular type of polarization of light and the model of study has to be made of a birefringent non-opaque material. In this sense, we aimed the creation of a low-cost transmission polariscope built-in MDF and polarizing films. To enable the films to be rotated together or separately, it was decided to insert step motors connected to an Arduino UNO board. Submitting a model based on the resin to a diametrically applied tension and analyzing the images, the photoelastic constant is quantified. The experiment showed that the built structure and the method used are adequate for the visualization of photoelastic patterns and for quantitative and qualitative analysis at the educational level for teaching in Engineering, being possible to extend its application to research in different areas.*

Keywords: *transmission photoelasticity, stress analysis, birefringent material, plane polariscope, circular polariscope.*

1. INTRODUCTION

Photoelasticity is an already well-developed stress analysis technique used for models with complicated geometry, complicated loading conditions, or both. In cases where mathematical methods can be cumbersome and tiring the use of, experimental observation and analysis becomes more appropriate technique for a qualitative and quantitative investigation of stress levels.

This type of analysis allows an interaction between the most different areas of experimental research, such as in dentistry that uses the photoelasticity technique to evaluate the tensions caused by loading in implants. Anami et al. (2015) emphasize the importance of photoelasticity because it allows the visualization of the stress distribution, which is important to understand the transfer of masticatory loads to the implant around the bone, a crucial biomechanical factor for bone-integration and fundamental for rehabilitation treatment to be successful.

Recently, Lherminier et al. (2019) produced an experiment that uses photoelasticity to visualize the lines of force through a granular layer in the shear test capable of sharing many qualitative similarities with the seismic dynamics.

The technique of photoelasticity can be of transmission or reflection, where the former studies samples and the latter indicated for prototypes. In this work, a polariscope is constructed to study photoelasticity by transmission in epoxy resin based samples. With the creation of a polariscope, a differentiated approach is possible in the analysis of internal efforts not only analytically, but also experimentally, by narrowing the relationship between the student and the object of study. In Engineering, the students learn theoretical concepts and formulations, while with the application of the photoelasticity method, they incorporate a physical and visible sense to the mathematical concepts related to stress and tensions. Understanding, in terms of tensions, related to the performance and strength of a structure that is subject to the various types of efforts, therefore becomes complete and productive.

Given the potential use of the technique for teaching and research, including the high cost of the polariscopes, the purpose of this paper is to provide an efficient, low-cost plane or circular polariscopes, useful for qualitative and quantitative experimental stress analyzes.

2. PRINCIPLES OF THE PHOTOELASTICITY THEORY

A polariscope uses the photoelasticity properties of a material to obtain the difference between the principal stresses ($\sigma_1 - \sigma_2$) and its orientation at each point along with the entire sample, which in this case will be a transparent polymer based material.

Optically isotropic polymers under normal conditions, when subjected to a tension, change the polarization of the light that crosses it, causing double refraction. This phenomenon is known as birefringence. It means the sample behaves like a crystal when compressed, allowing the experimental analysis of stress in models.

Since light is the primary tool for photoelasticity, it is necessary to understand how it behaves. According to Maxwell's Electromagnetic Theory, light is an electromagnetic wave formed by two fields of vectors, one electric (E) and the other magnetic (B), Fig. 1a, both in phase, with the same direction of propagation and perpendicular one to another. In order to make the mathematical description, for sake of simplicity we can choose any one of these vectors. In our case we choose the electric field (Fig. 1b) whose magnitude in a specific instant is given by

$$E = A \cos\left(\frac{2\pi}{\lambda} ct\right) = A \cos(2\pi ft) = A \cos \omega t, \quad (1)$$

where λ is the wavelength, ω is the angular frequency, f is the linear frequency, c is the propagation velocity, t is the time, and A the amplitude of the light.

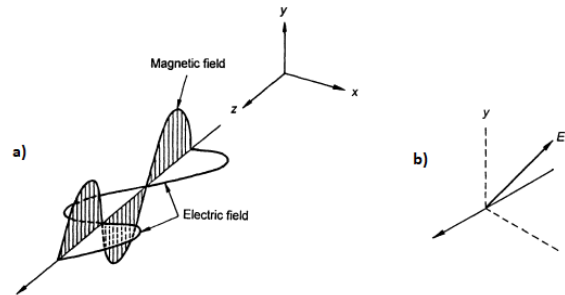


Figure 1. a) The electric and magnetic vectors associated with an electromagnetic wave b) Representation of light as a vector.

Available from: Ramesh (2000)

As for the polarization of light used in the polariscope, three main types of polarization will be used as illustrated in Figure 2. The first case, shown in Fig.2a, we have a circularly polarized light, where two orthogonal planes containing polarized light of the same amplitude and a phase difference of one-quarter of the wavelength ($\delta = \lambda/4$) result in a rotating wave with constant angular amplitude and frequency. The second, in the Fig.2b, is the case of elliptically polarized light that occurs when two plane-polarized light waves have different amplitudes and a phase difference δ . Finally, one obtains the plane-polarized light in the Fig.2c when all vectors of the arbitrary amplitude of all light rays are strictly oscillating in a single plane, not necessarily vertical.

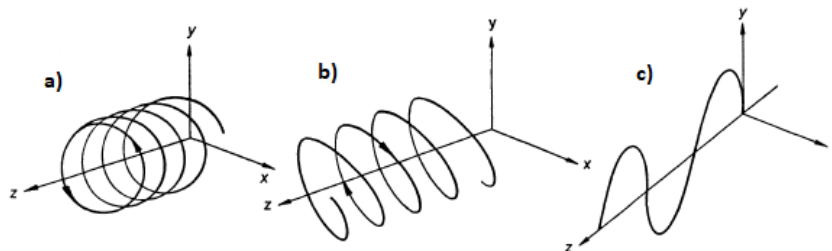


Figure 2. Light a) Circularly polarized b) Elliptically polarized c) Linearly polarized.

Available from: Ramesh (2000)

For the application of the photoelasticity method, it is necessary to obtain polarized light in a plane from natural light using polarizing filters, available for purchase in the form of sheets in various sizes. Polarizing filters act as a polarizer by letting only one component of incident light pass in a single direction parallel to its polarization direction. The reason for this is because they are dichroic materials, that is, they absorb polarized light in a direction with more intensity than

polarized lights perpendicular to this direction, as can be seen in Fig.3. The two types of polariscope, whose description is the following, will use these polarizing filters.

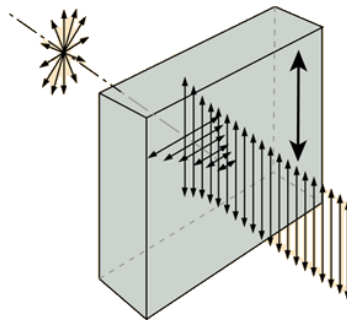


Figure 3. Dichroic material acting as a polarizer.

Available from: <http://hyperphysics.phy-astr.gsu.edu/hbasees/phyopt/polabs.html>

2.1 Plane Polariscope

A polariscope is an optical instrument used to analyze birefringence in samples. Depending on the configuration, one can set up a plane polariscope and circular polariscope. In this section, we will deal with the first one.

The plane polariscope consists of a light source, followed by a polarizer, a sample holder with the ability to introduce stress on the object of study, and a second polarizer, perpendicular to the first, known as the analyzer, as shown in Fig.4.

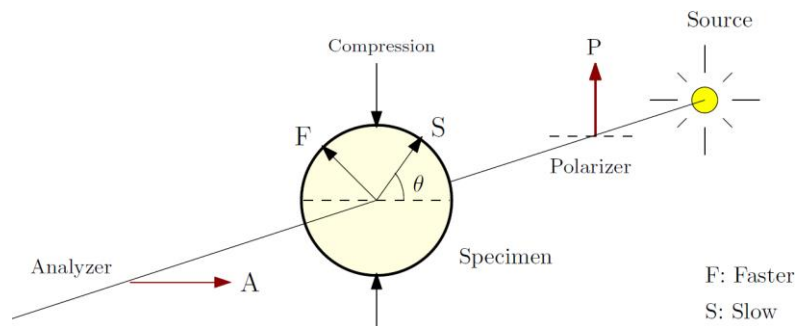


Figure 4. Plane polariscope.

In order to understand what happens with light passing through the plane polariscope, consider the scheme of Fig. 4. The applied tension in the sample will develop a plane state of stress at each point, characterized by the principal stresses σ_1 and σ_2 . Thus, linearly polarized light coming out of the polarizer, when arriving in the sample, is divided into two components in the direction of the principal stresses at each point of the sample, each with a different refractive index. The difference in refractive index causes the light to travel at different speeds in each polarization. This is the phenomenon known as double refraction or birefringence previously mentioned. These two rays originated from birefringence are known as ordinary and extraordinary rays. The extraordinary ray is the one along the F axis, having a lower refractive index (n_2), then with a higher velocity, while the ordinary one follows the S axis, having a higher refractive index (n_1), then with a slower speed. Since both remain in the same direction of propagation, this difference in velocity causes only a delay between the phase of the two waves. According to Ramesh (2000), the phase (δ) between the two waves relates to the refractive indices of the rays at each point of the sample through the equation

$$\delta = \frac{2\pi h}{\lambda}(n_1 - n_2), \quad (2)$$

where h is the thickness of the sample. From Equation 2, we notice that for a given thickness, the phase difference depends on the wavelength.

After the extraordinary and ordinary rays emerge from the sample with a relative delay, they go to the analyzer which transmits only the components along its axis. Also, as detailed by Ramesh (2000), the intensity of the light coming out of the polariscope, that will be analyzed, is given by

$$I = I_{Ri} \sin^2 2\theta \sin(\omega t) \sin^2 \left(\frac{\delta}{2} \right), \quad (3)$$

with I_{Ri} meaning the intensity of the incident ray on the sample.

From Equation 3, one can see that the observer will not see the light passing through the sample at a given point under two conditions. The first one, $\sin^2 2\theta = 0$, occur when $\theta = m\frac{\pi}{2}$, with m an integer (0, 1, 2...), which indicates that all regions of the sample where the direction of some principal stress coincides with that of the polarized axis will be seen dark. The locus of these points is called *isoclinic*, where the slope (θ) of the principal stresses is the same for all points in that region, which appears dark in Fig. 5b when use white light and in Fig. 5a when use monochromatic light. The isoclines are independent of the wavelength and do not change with the increase of load, since in the linear elasticity, when adding the load only the magnitude of the stress changes, but not its orientation.

The second condition occurs when $\sin^2 \delta/2$, that is, $N = \delta / 2\pi = n$, with n an integer (0, 1, 2...), and N the fringe number. The term used for the fringes under these conditions is *isochromatic*, which, as detailed by Ramesh (2000), are related to the principal stresses by the following equation

$$(\sigma_1 - \sigma_2) = N \cdot f_\sigma / h, \tag{4}$$

where f_σ the constant of fringe or *material stress fringe value* given in units of $N/mm.fringe$. To obtain the difference between the principal stresses at the points of interest of the sample, knowing the fringe constant of the material, one must assign the order number related to each point of interest (Dally and Riley, 1991).

Thus, as is expressed by Eq. (4) and Eq. (5), the isochromatic occurs when the difference between the principal stresses ($\sigma_1 - \sigma_2$) is such that the relative phase difference is $2n\pi$ (where n is an integer). The isochromatic only appear dark when using a monochromatic light source where the wavelength is unique, Fig. 5a. When using white light, only the first isochromatic fringe appears dark, Fig. 5b.

It is worth noting that in practice, isoclinic cannot be obtained alone without the presence of isochromatic, not all the isoclinic contours can be obtained in a single photo; it is necessary to rotate the polarizer and analyzer (remaining crossed) to obtain the isoclinic ones along with sample through the plane polarizer.

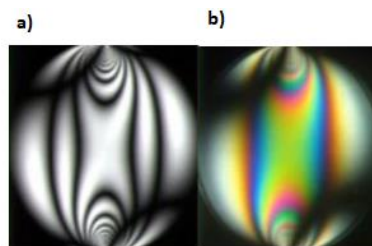


Figure 5: The image formed in the plane polariscope by the use of a) monochromatic light b) white light.
 Available from: <https://nptel.ac.in/courses/112106068/15>

2.2 Circular Polariscopes

The circular polariscope is composed of a white or monochromatic light source, a polarizer followed by a quarter-wave filter incident on circularly polarized light in the stressed sample, which after the sample passes by the second filter of a quarter-wave crossed over the first, to reach the analyzer (Fig. 6). This arrangement can have two configurations: if the axis of polarization of the analyzer are perpendicular to the axis of the polarizer as shown in Fig. 6, we say that it is a dark-field, obtaining images as in Fig. 7a, if the axes are parallel to each other we say that it is a light-field, obtaining images as in Fig. 7b. We will follow the explanation considering the arrangement of the circular polariscope to dark field.

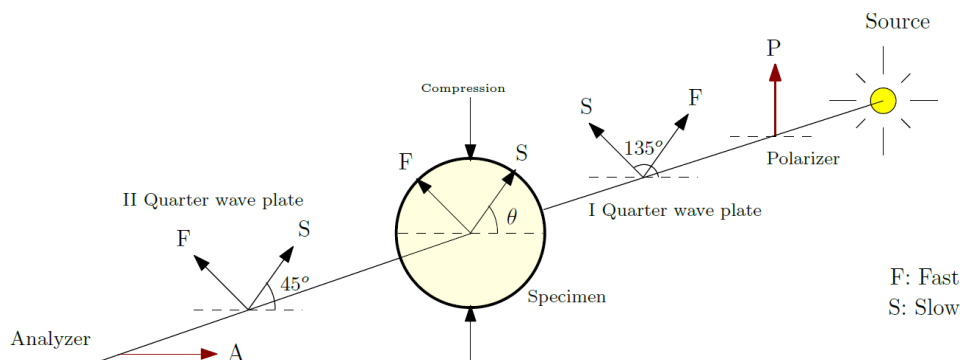


Figure 6. Circular Polariscopes.

In the plane polariscope, when the polarized light coincides with one of the reference axes at given points in the sample, there is the production of isoclines. On the other hand, when the incoming light is circularly polarized, the extinction of light due to the dependence of the direction of the principal stresses does not exist anymore, which can easily be perceived by analyzing the following equation of light intensity for the dark field:

$$I = I_{Ri} \sin^2 \frac{\delta}{2}, \quad (5)$$

where dark fringes will arise for $\delta = 2m\pi$, where m is an integer (0, 1, 2...).

One can see from Eq. (5) that the intensity of the light emerging from the circular polariscope does not have the term θ , that is, in the circular polariscope do not obtain isoclinic, only isochromatic.

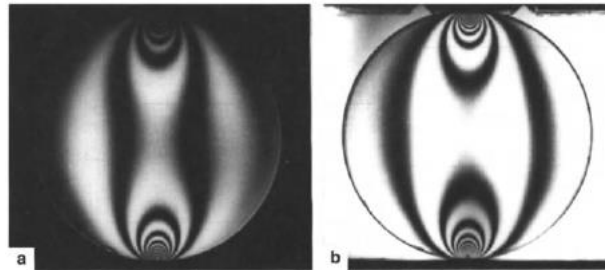


Figure 7. a) Dark field image b) Light field image.
Available from: Ramesh (2000)

The second quarter-wave filter works to cancel the delay inserted by the first since its axes have the same amplitude but crossed directions. Thus, Ramesh (2000) says that the arrangement with crossed quarter-wave filters is preferable in order to minimize the influence of the error due to their use.

3. METHODOLOGY

3.1 The Polariscope

As the polariscope structure is composed of two polarizers and two $\frac{1}{4}$ wave filters, we chose to make two equal and independent support structures, each having a polarizing filter on one side and a $\frac{1}{4}$ wave filter on the other. In order to cheapen the project, it was decided to make the construction using MDF. In the main part are coupled two bearings and a step motor responsible for the support of the central disc containing the polarizing film and by rotation thereof, Fig. 8. In order to ensure accurate rotation of the polarizers, a stepper motor is present in each part of the structure connected to an Arduino UNO board and a ULN2003 driver (that allows Arduino to control the motors with currents higher than 50 mA).

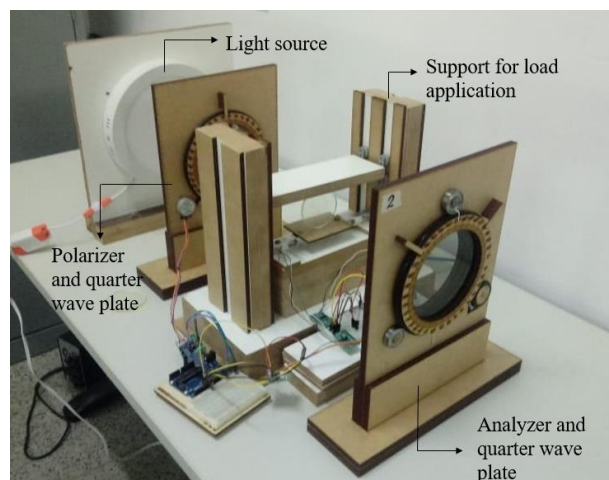


Figure 8: Experimental setup.

For the rotation of the central disc, it is necessary an arrangement in which two o-rings are placed in contact (one in the engine and one in the central circle) and slide over two bearings that also make the support in the central part.

Using the diameter of the two discs, one can find a transmission ratio of about 0.24. Because differences in the assembly and confection of the pieces are inevitable, for each set, there will be a correspondent relation. The values were recorded in the physical demarcation of the primary disk (G-angle) each time the motor rotated 20° (Angle P) and was named as "Polarizer 1" and "Polarizer 2" to differentiate the two structures. As a result, we obtained two graphs (Fig. 9 and Fig. 10) showing the relationship between the data, i.e., the corresponding curve, as well as the equation (y) equivalent to the transmission ratio. The transmission ratio allows changing the motor program so that it rotates according to the desired number of degrees for the central disc.

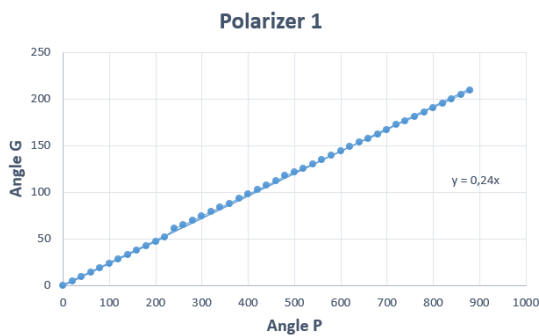


Figure 9: Polarizer transmission ratio 1.

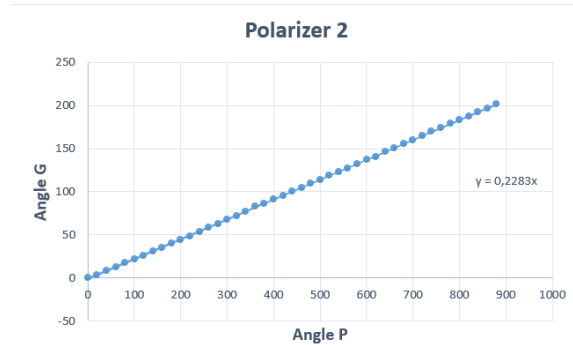


Figure 10: Polarizer transmission ratio 2.

The raw material of the support used to compress the sample is Medium Density Fiberboard (MDF). The weights used for compression are iron plates that range from 0.920 kg to 2 kg. The support has two load cells, with an HX711 module each, to measure the load applied to the sample and permit to obtain the constant of fringe (f_σ). It is essential to guarantee a good connection among the load cells and the Arduino UNO board.

3.2 Manufacture of photoelastic models

The molds to produce the photoelastic models were made of silicone rubber (Fig. 11) in the mass proportions indicated by the manufacturer (100% silica to 03% catalyst). An acrylic disc with 60 mm diameter and 4 mm thickness is the reference for a negative mold. Fig. 12 shows the obtained result.



Figure 11: Silicone rubber.



Figure 12: Mold and negative used.

For the preparation of the model, one uses the rigid epoxy resins "2001" (Fig. 13) and flexible SQ - 2220 (Fig. 14) and follows the manufacturer's recommendations (100% resin to 50% bulk hardener). However, for blending the properties of the rigid and flexible resins, 70% of the rigid was mixed with 30% of the flexible (along with the indicated ratio for the hardener). For the quantities to be as precise as possible, we use a precision scale. The material was mixed calmly and transferred to the mold in order to fill the whole space without sudden changes in the flow. This careful procedure is to avoid the formation of bubbles, which would make it difficult to visualize the photoelastic patterns, and to avoid points of concentration of tension. In this way, we obtained a resin disc with the same dimensions of the negative used. Initially, the material showed to be uniform and transparent, fundamental characteristics for a proper application of the photoelastic technique.



Figure 13: Epoxi resin 2001 with hardener.



Figure 14: Epoxi resin SQ – 2220 with hardener.

3.3 Polariscope calibration

An indispensable step for photoelasticity experiments is the calibration of the polariscope used for the analyzes. It means to establish the orientations of the polarizer axes and the $\frac{1}{4}$ wave filters. For the construction of the polariscope, the directions of polarization of the polarizer and analyzer were known. In this way, one can rotate the polarizer relative to the analyzer until obtaining the complete extinction of light.

However, the directions of the transmission axis of the waveplates were unknown and therefore needed to be determined. The step-by-step approach of Cloud (1998) is:

(a) One of the quarter wave plates should be positioned between the polarizer crossed with the analyzer and rotated until extinction is achieved. In this position, the transmission plates of the wave plate are aligned with the transmission axis of the polarizer and the analyzer. The given procedure does not tell us which of the two axes is the fast axis in the wave-quarter plate.

(b) To determine the positions of the axes for the second wave plate, one must remove the first one and perform the same procedure.

When one places the wave-quarter plates on the polariscope between the polarizer and the analyzer, a small amount of light will pass through the analyzer, or, in other words, it absorbs a relatively large amount of light. With the monochromatic light, whose wavelength corresponds to the design of the wave plate, the small intensity of the light must be zero (i.e., it reaches extinction). On the other hand, if the wavelength of the light does not correspond to the quarter-wave plates, or if using white light (polychromatic source), a minimal amount of transmitted light (rather than extinction) will be observed. If the initial positioning of the waveplates results in minimal light transmission, then the two fast shafts of the wave-quarter plates are in opposition, which is the correct arrangement. However, if a large amount of light is transmitted, to achieve minimum transmission, it is necessary to rotate any of the quarter-wave plates by 90° . These guidelines must be marked so that the plates can be removed and reinstalled with their crossed spindles.

With the transmission axis of the quarter-wave plate arranged so that they are at 45° from the polarizer and analyzer axis, there is the conversion of the linear polariscope to circular. To reach this state, it starts with the linear arrangement obtained earlier and rotates both $\frac{1}{4}$ wave filters in the same direction 45° .

4. RESULTS

4.1 Obtaining the photoelastic constant

After all the steps of preparation of the material and calibration of the structure, one can then start the experiments. A widespread analysis is to determine the constant of the fringe of the material, $f(\sigma)$, from a disk (made from the same material for other tests) under diametrical compression.

Knowing that the principal tensions in a disc under diametrical compression given by Timoshenko's theory of elasticity (1957) is:

$$\sigma_x - \sigma_y = \frac{8P}{h\pi D} \cdot \frac{D^4 - 4D^2x^2}{(D^2 + 4x^2)^2} \quad (6)$$

where P is the applied concentrated load, D is the disk diameter, and x is the location of the point of interest on the disk. In this way, replacing Eq. (4) in Eq (6), we obtain for the fringe constant in the center of the disk ($x = 0$):

$$f(\sigma) = 8P/\pi DN \tag{7}$$

where N is the fringe order passing through the center of the disk. The point chosen to obtain the fringe constant was in the center of the disk in order to simplify the calculations of Eq (6).

The values of P are obtained with high precision since the structure for the application makes use of two load cells in the support shown in Figure 8. For the experiment to be more precise, one uses the Tardy compensation method explained by Ramesh (2000) while adding the load the values to register the value of N. The measured values are in Table 1. The linear relationship between the load and the fringe number in the center of the disk, shown in the graph of Fig. 15, can be determined. This same behavior (linear relationship) is seen in the construction work of a polariscope by Silva et al. (2008).

Table 1: Values of P and the corresponding N.

P [Newtons]	0,000	19,22(8)	28,09(5)	38,96(6)	48,36(3)	57,38(8)
Fringe Number	0,000	0,816	1,216	1,616	2,372	2,666

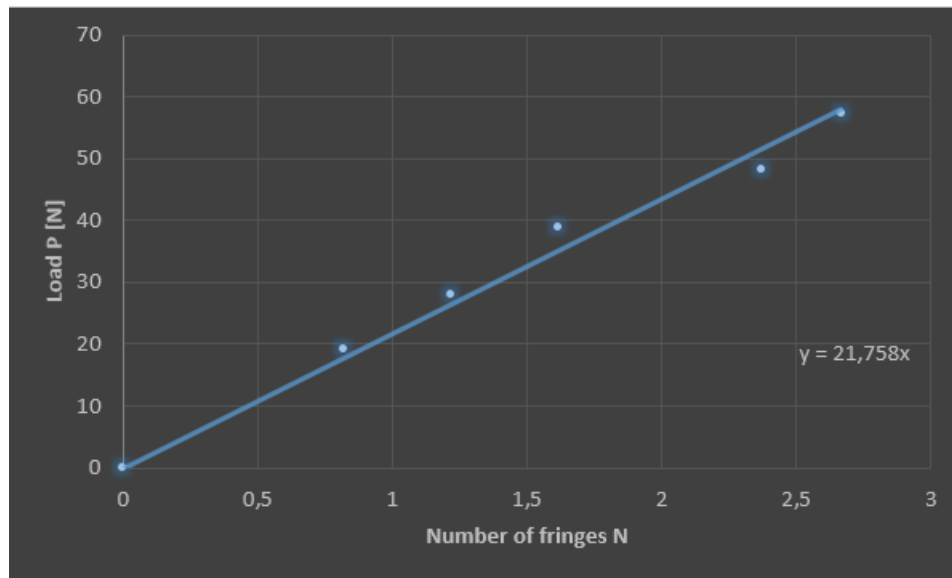


Figure 15: Graph to obtain the P/N ratio.

With the geometric data corresponding to the model used in the experiment and the relation established for P and N, it was possible to determine the value of $f(\sigma)$ by Eq. (7):

$$f(\sigma) = 0,923 \text{ N/mm} \cdot \text{fringe}.$$

With $f(\sigma)$, it is possible to obtain the stresses differences at each point of the sample by using Eq. (4) once the fringe number of the point to be analyzed and the thickness of the sample is known.

The method was efficient and allowed the constant value to be used to carry out quantitative tests with an acceptable margin of error in samples made from the same material and according to the ratio used to manufacture the calibration disk.

4.2 Photoelasticity tests

First, the photoelastic sample was visualized in the plane polariscope with no loads to observe the possible presence of internal stresses and edge effect from the fabrication and curing of the model. The images were obtained using a *Nikon P900* camera; however, it is possible to get the same results with any good digital camera or cell phone. The sample was completely transparent and free of tensions (Fig. 16), a characteristic desired for a better application of the technique.

Also, in the plane polariscope, to test the sensitivity of the material, a small arbitrary load was diametrically applied. It is clear the points of concentration of tension at the points of contact with the structure responsible for the application of force, as shown in Fig.17.



Figure 16: Sample without load on the plane polariscope

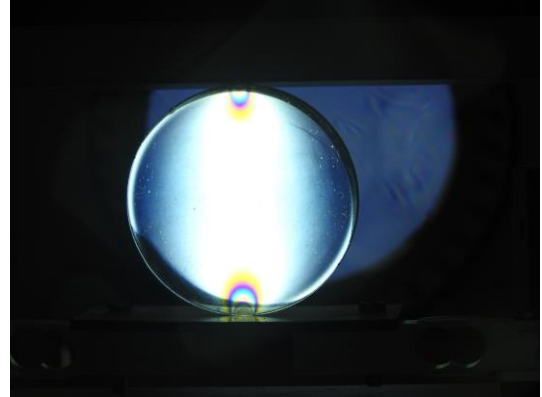


Figure 17: Sample with low load on the plane polariscope.

The fringes appear from the ends to the center of the disc in response to the increased force applied to reveal various isochromatic patterns, as well as the isoclinic patterns. To verify different isoclinic patterns, we started with the polarizer and analyzer with their polarization axes crossed each other as shown in the scheme of Fig. 4, obtaining the image of Fig. 18, then, the polarizer apparatus was rotated so that they remained perpendicular to each other. Fig. 19 shows the isoclinic corresponding to a rotation of 30° clockwise concerning horizontal.

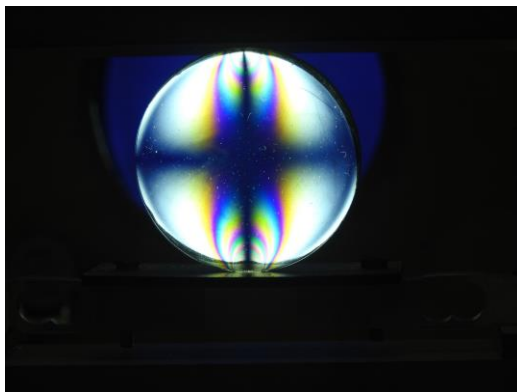


Figure 18: Sample with isochromatic and isoclinic on the plane polariscope.

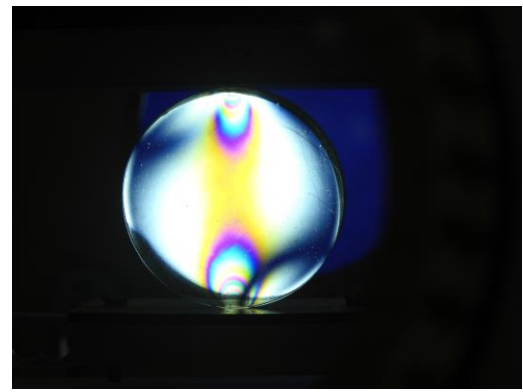


Figure 19: Sample with isochromatic and isoclinic at 30° on the plane polariscope.

In the circular polariscope, the isoclinic patterns are extinct because there is no more dependence on the principal stress directions, presenting only isochromatic patterns, as can be seen in Fig. 20:

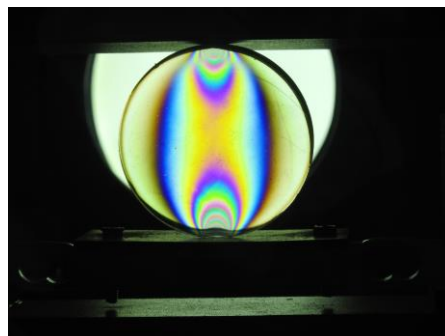


Figure 20: Sample on the circular polariscope.

Thus, the analyzes made in the polariscopes in both the plane and circular configurations were coherent because the presented fringe patterns follow the same standards presented by Freddi, Olmi, and Cristofolini (2015) when they address the introduction to photoelasticity.

Since the studies of solid mechanics and resistance of materials are crucial in Engineering courses, it is essential to have available a polariscopes structure that can be taken to the classroom and providing a visual analysis of stress concentrations and its distributions. Due to the easy manipulation of the resins used, it is possible to create several types of models to observe different kinds of reactions to mechanical stress in a full field analysis providing more active learning in the academic environment.

5. CONCLUSION

The results obtained in this article prove the academic potential of the structure built for Teaching the experimental technique of photoelasticity. Such a structure allows the plane and circular polariscopes configurations to obtain the differences between the principal stresses and their respective orientations for each point of the compressed sample, as well as a qualitative analysis of the distribution of these stresses.

6. REFERENCES

- Anami, L.C., et al., 2015. "Stress distribution around osseointegrated implants with different internal-cone connections: photoelastic and finite element analysis". *Journal of Oral Implantology*, Vol. 41, No. 2, pp. 155–162.
- Cloud, G., 1998. *Optical methods of engineering analysis*. Cambridge university press.
- Dally, J.W. and Riley, W.F., 1991. *Experimental stress analysis*. McGraw-Hill Book Company, New York, 3rd edition.
- Doyle, J.F., Phillips, J.W and Post, D., 1989. "Manual on Experimental Stress Analysis". *Society for Experimental Mechanics*.
- Freddi, A., Olmi, G., Cristofolini, L., 2015. *Experimental Stress Analysis for Materials and Structures: Stress Analysis Models for Developing Design Methodologies*. Springer, Switzerland, 2015.
- Lherminier, S. et al., 2019. "Continuously sheared granular matter reproduces in detail seismicity laws". *Physical Review Letters*, Vol. 122, No. 21.
- Ramesh, K., 2000. *Digital Photoelasticity: Advanced Techniques and Applications*. Springer, 1st edition.
- Schiavon, J.A., 2010. *Aplicação da técnica da fotoelasticidade na análise de fundações por estacas helicoidais*. Master's thesis, Universidade de São Paulo, São Carlos, Brasil.
- Silva, J.P., Araújo, C.A., Oliveira, S.G. and Sousa, M.M., 2008. "Projeto e construção de um polariscópio portátil utilizado na técnica da fotoelasticidade de transmissão plana". *V Congresso Nacional de Engenharia Mecânica – CONEM 2008*. Salvador, Brasil.
- Timoshenko, S., 1957. *Resistencia de los Materiales*. Espasa-Calpe S.A, Madrid.

7. ACKNOWLEDGMENT

We are grateful to the Mechanical Engineering course of the Federal University of Piauí for providing the facilities for the conduction of the experiments. The authors also acknowledge the financial support by the Brazilian agency National Council for Scientific and Technological Development (CNPq).

8. RESPONSIBILITY NOTICE

The authors are the only responsible for the printed material included in this paper.